Cell PRESS

Sensing sound: molecules that orchestrate mechanotransduction by hair cells

Piotr Kazmierczak and Ulrich Müller

Dorris Neuroscience Center, Department of Cell Biology, The Scripps Research Institute, La Jolla, California 92037, USA

Animals use acoustic signals to communicate and to obtain information about their environment. The processing of acoustic signals is initiated at auditory sense organs, where mechanosensory hair cells convert sound-induced vibrations into electrical signals. Although the biophysical principles underlying the mechanotransduction process in hair cells have been characterized in much detail over the past 30 years, the molecular building-blocks of the mechanotransduction machinery have proved to be difficult to determine. We review here recent studies that have both identified some of these molecules and established the mechanisms by which they regulate the activity of the still-elusive mechanotransduction channel.

Introduction

Our ability to perceive sound is a demonstration of the extreme signal processing capability of the nervous system. The mammalian auditory system responds to sound-induced vibrations at atomic dimension, can amplify signals >100 fold, and has a wide dynamic range that enables us to perceive sound over a large intensity and frequency range. Changes in air pressure induce fluid motions that travel along the cochlear duct and induce mechanical vibrations at the sensory epithelium in the organ of Corti (Figure 1a,b). As a consequence of gradual changes in the physical properties of the cochlea from the base to the apex, each segment of the sensory epithelium vibrates in response to a specific frequency. Three rows of outer hair cells (OHCs) (Figure 1b) amplify the vibrations. The mechanical signals are then transferred onto inner hair cells (IHCs) (Figure 1b), which transmit the information to afferent neurons. Hair cells at the base of the cochlea respond to the highest frequencies and those at the apex to the lowest. Sound frequencies are therefore relayed to the nervous system as a tonotopic map ([1–4] for recent reviews).

At the heart of hearing is the mechanotransduction process, the conversion of mechanical force into electrical signals. This process is carried out by the mechanosensory hair cells of the cochlea. The molecular components of the mechanotransduction machinery of hair cells have for decades escaped detection, largely because hair cells are few in number and hard to manipulate experimentally. As in other experimental systems, genetic studies have recently overcome these problems. The study of genes that are linked to deafness, the most common form of sensory impairment in humans, has finally led to the identification of some of the components of the mechanotransduction machinery. Here we summarize these findings as well as several studies that have provided insights into the properties of the molecules of mechanotransduction.

Auditory mechanosensation: converting sound into electrical signals

Hair bundles and tip links

The mechanically sensitive organelle of a hair cell is the hair bundle, which consists of actin-rich stereocilia that contain mechanotransduction channels close to their tips (Figure 1c, Figure 2a,b). Stereocilia are organized in rows of decreasing heights and are connected by extracellular filaments, including the tip and ankle links, and also the top-connectors (Figure 2a). These linkages are remodeled during development; mature murine cochlear hair cells retain only tip links and top connectors ([3,4] for recent reviews). The stereociliary bundle is polarized in the apical hair cell surface, which provides directional sensitivity to stimulation. Sound-induced deflection of the hair bundle in the direction of the longest stereocilia increases channel open probability; deflections in the opposite direction decrease channel open probability ([1] for recent review).

Since their original discovery [5], tip links have been proposed to transmit tension force onto the transduction channel. In support of this model, tip links are oriented along the mechanical sensitivity axis of hair cells [5]. Furthermore, Ca^{2+} flows into sterocilia close to their tips [6,7]. Finally, disrupting tip links by removal of Ca^{2+} or treatment with the protease elastase leads to loss of mechanosensitivity of the hair bundle [8,9].

Coherence in motion

The hair bundle of a hair cell is exquisitely sensitive to mechanical stimulation. At the threshold of hearing, bundles are deflected by <1 nm [10,11]; maximal response to mechanical stimulation is evoked by $\sim 1^0$ angular deflection [12]. The analysis of hair-bundle motion in response to low-frequency stimulation has shown that stereocilia tilt around the pivots at their base [13–15]. Recent optical measurements with frog saccular hair cells demonstrate that the stereocilia within a bundle show a high degree of coherence in motion with little splay [16,17]. Pretreatment of hair bundles with the Ca^{2+} chelator, BAPTA, to break tip links

Corresponding author: Müller, U. (umueller@scripps.edu).

 0166-2236/$ – see front matter doi:10.1016/j.tins.2011.10.007 Trends in Neurosciences, April 2012, Vol. 35, No. 4

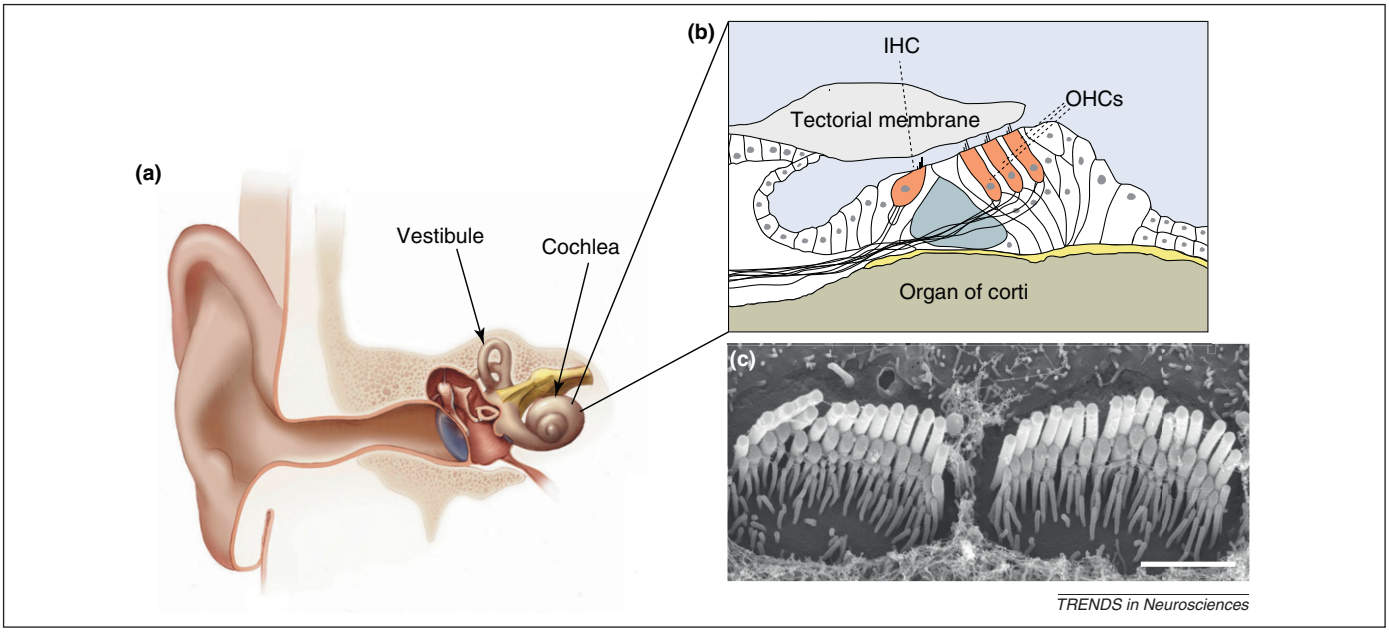

Figure 1. The mammalian auditory sense organ and its hair cells. **(a)** Diagram of the inner ear. The snail-shaped cochlea (end-organ for the perception of sound) and parts of the vestibule (end-organ for the perception of head movement) are indicated (panel modified from [4]). **(b)** Diagram of the organ of Corti. One inner hair cell (IHC) and three outer hair cells (OHCs) are indicated. **(c)** Scanning electron micrograph of the cochlear sensory epithelium of the mouse after removal of the tectorial membrane (kindly provided by Dr Nicolas Grillet, The Scripps Research Institute). The image shows the stereociliary bundles of two IHCs. Note the staircase arrangement of the rows of stereocilia. Scale bar, 2 μm.

[16,17], or with proteinase XXIV to remove ankle links and shaft connectors [16], does not affect coherence in motion. These treatments leave top connectors intact, suggesting that they might mediate sliding adhesion between stereocilia [16,17]. At small deflections, the close apposition of stereocilia immobilizes the liquid between them, and this reduces drag in the bundle and suppresses the squeezing but not the sliding mode of stereociliary motion. Therefore, most stereocilia inside the bundle experience little viscous drag; their tips experience maximal force [18]. Coherence in stereociliary motion ensures excellent sensitivity to mechanical stimulation by allowing for synchronous gating of transduction channels across the bundle.

Transducer channel activation

Transduction channels open in response to mechanical stimulation within microseconds, indicating that mechanical force directly gates the channel [12,13]. In the turtle, activation kinetics vary tonotopically [19]; it is reasonable to assume, although not experimentally verified, that tonotopic variation is a universal feature of the vertebrate cochlea, thereby matching the properties of the transduction channel to the sound frequency they process. The properties of the transducer current fit well with a model where mechanical force is transmitted to the molecular gate of the transduction channel by an elastic gating spring with a stiffness of ~1mN/m [12]. Deflection of the hair bundle towards the longest stereocilia increases tension in the gating spring, and this promotes channel transition from the closed to the open state (Figure 2c) [20]. Based on the mechanical behavior of hair bundles, the length of the swing by the gate of the transduction channel is estimated to be ~4–11 nm [21,22]. This is a relatively large displacement and might reflect conformational changes in more than one molecule.

Transducer channel adaptation

Following activation, hair cells adapt to constant mechanical stimulation. Adaptation is thought to extend the dynamic range of hair cells, contribute to their frequency selectivity, and assist in signal amplification. In the absence of mechanical stimulation, adaptation also establishes a resting current in hair cells ([1,23–25] for recent reviews). Adaptation progresses on a fast and slow time-scale and is regulated by influx of Ca^{2+} through the transduction channel [26,27] (Figure 2c). Adaptation in the cochlea is faster than in the vestibule, and fast adaptation rates vary tonotopically where cells responding to higher frequencies show higher adaptation rates [19,26,28–34]. These features of adaptation are probably important for tuning hair cells to their specific frequencies.

Fast and slow adaptation are thought to take place by different mechanisms (Figure 2c). Two prominent models have been proposed for fast adaptation. In one model, Ca^{2+} binds to the channel and stabilizes it in the closed state [21,35]. Alternatively, Ca^{2+} might bind to a site near the channel, causing release of a mechanical element in series with the transduction machinery leading to decrease in tension and channel closure [36,37]. Slow adaptation is thought to involve an adaptation motor linked to the upper insertion point of tip links. According to the model, the motor protein climbs up along F-actin, establishing tension in the transduction machinery. During mechanical stimulation, Ca^{2+} that flows into stereocilia releases the motor from F-actin, reducing tension and leading to channel closure. Subsequently, the Ca^{2+} concentration in stereocilia declines and the motor re-establishes tension (Figure 2c) [38,39]. As outlined below, recent studies suggest that models of slow adaptation might need revision.

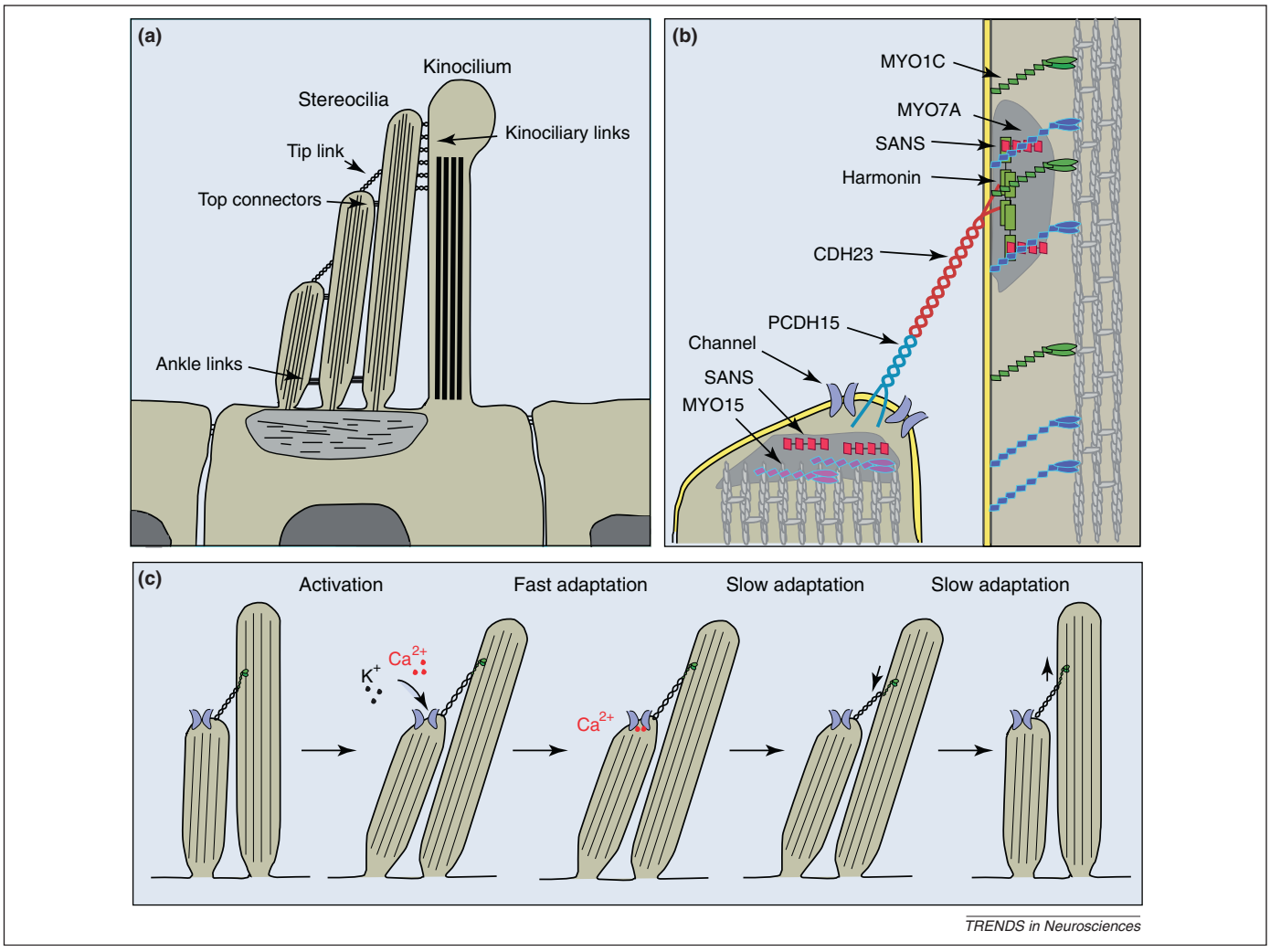

Figure 2. Hair cells and their mechanotransduction machinery. **(a)** Cross-section through the apical part of a hair cell. Hair bundles consist of several rows of actin-rich stereocilia and a microtubule-based kinocilium. The sterocilia are connected to each other and to the kinocilium by extracellular filaments that can be visualized by electron microscopy. These are the tip links, top connectors, ankle links and kinociliary links ([4] for recent review). Note that the kinocilium, kinociliary links, ankle links and top connectors are present in murine cochlear hair cells only during hair-bundle development. These structures degenerate once hair bundles have reached their mature shape and only stereocilia, tip links and top connectors remain [113]. **(b)** Diagram of the tip-link region, indicating molecules that are part of the tip-link complex. CDH23 homodimers form the upper part of the tip link and PCDH15 homodimers the lower part [58]. Two electron-dense regions (shaded in grey) can be visualized by transmission electron microscopy in proximity to the upper and lower insertion sites of tip links [102]. Immunolocalization studies have localized the indicated proteins to the electron dense regions ([4] for recent review). **(c)** Current model of activation and adaptation of transduction channels in hair cells. Transduction channels that are located in proximity to the lower insertion site of tip links are opened by deflection of the hair bundle in the direction of the longest sterocilia. The tip link is thought to gate the channel. Ca^{2+} that flows into the stereocilia leads to fast adaptation probably by binding to the channel or a molecule nearby. Slow adaptation is thought to be regulated by a myosin motor complex at the upper insertion site of tip links. Upon Ca^{2+} entry, the adaptation motor is released from the cytoskeleton and slips down the actin filaments, leading to channel closure. Tension in the transduction complex is restored by movement of the myosin motor towards the tips of stereocilia ([1] for recent review). However, the localization of the transduction channel raises questions regarding models of slow adaptation because it places the site of Ca^{2+} entry into stereocilia at the lower tip-link end, far away from the proposed localization of the adaptation motor at the upper tip-link end. It has been proposed that Ca^{2+} entering through the transduction channel might affect the adaptation motor hooked up to the next tip link lower down in the same stereocilium [1], but adaptation motors in the longest stereocilia would then probably not show Ca^{2+}-dependent adaptation.

The elusive transduction channel

Channel numbers and properties

Despite decades of study, the hair cell's transduction channel has not been identified. The challenges to identify the channel are tremendous. Most importantly, there are few hair cells and transduction channels per animal. Hair cells also resist experimental manipulations typically used in other experimental systems. For example, hair cells are difficult to transfect, necessitating time-consuming genetic studies to verify channel candidates. However, electrophysiological recordings have shown that the transduction channel is a non-selective cation channel with a preference for Ca^{2+} [40,41]. Best estimates suggest that there are two active channels per tip link [7,21,42,43]. Studies in the turtle indicate that the channel pore is considerably larger than in other cation channels with a minimal pore diameter of ~12.5 Å [44]. In the rat, channel conductance in IHC is in the order of 260 pS; it varies tonotopically in OHCs from 145 pS at the apex and 210 pS in the mid-frequency range and was estimated to be 320 pS in the high-frequency range [42]. Similar tonotopic conductance changes are observed in the turtle [43], indicating that this is a conserved property of the auditory system. The conductance changes indicate that the channel might consist of several subunits with variations in subunit composition along the length of the sensory epithelium.

Channel localization and slow adaptation

Ca^{2+} imaging studies initially supported the location of the transduction channel on both tip-link ends [7], but a recent

study using high-resolution imaging provided convincing evidence that the channel is localized to the lower tip-link end [6]. The localization of the transduction channel suggests a physical connection to the tip link, but it does not necessarily have to be direct. The channels could be opened by the change in tension of the lipid bilayer, as has been suggested in other systems [45,46]. In this model the number of open channels depends on the distance of force propagation within the membrane; a large number of channels could be present in stereocilia provided that, on average, only two channels are opened simultaneously by membrane stretch.

The localization of the transduction channel raises questions regarding models of slow adaptation because it places the site of Ca^{2+} entry into stereocilia at the lower tip-link end, far away from the proposed localization of the adaptation motor at the upper tip-link end (Figure 2c). To reconcile these differences it has been proposed that Ca^{2+} entering through the transduction channel might affect the adaptation motor hooked up to the next tip link lower down in the same stereocilium [1]. In this scenario, adaptation motors in the longest stereocilia would experience minimal changes in Ca^{2+} and probably not show Ca^{2+}-dependent adaptation. In addition, slow adaptation rates in mammalian auditory hair cells are much faster than in vestibular hair cells and hair cells in other species [26,31,32,34,35] raising the question of whether the same mechanism controls slow adaptation in all hair-cell types.

The tip link: an unusual cadherin adhesion complex

Molecular constituents of tip links

The hunt for the molecular components of the tip link has been active for over 20 years. Recent studies finally have demonstrated that tip links are formed by cadherin 23 (CDH23) and protocadherin 15 (PCDH15), two cadherin superfamily members (Figure 2b). Hints that these proteins are important in hair cells came from the observation that mutations in their genes lead to deafness [47–54]. In mice, mutations in *Cdh23* and *Pcdh15* also lead to morphological hair-bundle defects [48,52,54], and zebrafish with mutations in *Cdh23* lack tip links [55]. Immunolocalization studies with an antibody to CDH23 demonstrated its presence at tip links [56]. Subsequently, PCDH15 was localized to tip links [57]. Using a combination of immunolocalization, biochemical and structural studies, it was finally shown that tip links are heterophilic adhesion complexes consisting of parallel CDH23 *cis*-homodimers interacting in *trans* with parallel PCDH15 *cis*-homodimers to form the upper and lower parts of tip links, respectively (Figure 2b) [58]. Subsequent studies have confirmed the localization of CDH23 and PCDH15 at tip links [59].

A new adhesion mode

As with classical cadherins, tip-link cadherins each contain an ectodomain largely composed of extracellular cadherin (EC) repeats that fold into immunoglobulin-like globular domains featuring two opposed β-sheets formed by seven β-strands. Three Ca^{2+} ions bind between the EC domains and stabilize cadherin structure. Classical cadherins have 5 EC repeats, whereas the longest isoforms of CDH23 and PCDH15 have 27 and 11 EC repeats, respectively (Figure 3a) ([60–63] for recent reviews). Classical cadherins are Ca^{2+}-dependent homophilic receptors, albeit with some affinity for closely related family members [62,64,65]. They form large adhesion complexes at adherens junctions [61]. The basic adhesive unit is a *trans* dimer comprised of opposing monomers [66–68]. Binding is achieved through EC1, where N-terminal β-strands are swapped between binding partners (Figure 4a,b) [66,67]. Classical type I cadherins have one Trp residue at amino acid position 2 (W2) that fits into a hydrophobic pocket on the opposing EC1 domain, whereas classical type II cadherins contain two Trps (W2 and W4) that fit into two binding pockets, enhancing binding affinity (Figure 4c) [69].

The tip-link complex differs significantly from the classical cadherin complex. A tetramer consisting of two *cis*-homodimers interacting in *trans* is the functional unit [58]. Trp2/4 are not conserved in EC1. Two laboratories have solved the structure of the first 2 EC domains of CDH23 [70,71]. The typical EC fold is maintained but a classic *trans*-binding interface is not (Figure 4d,e). Instead, polar residues at the N-terminus of CDH23 form a novel Ca^{2+}-binding motif (Figure 4e,f). The PCDH15 N-terminus also harbors polar amino acids; biochemical studies show that polar amino acids in both cadherins are required for *trans* binding [70]. These amino acids might be necessary for correct protein folding or could serve to integrate Ca^{2+} into the *trans*-binding surface, perhaps to increase adhesive strength. In classical cadherins the *trans*-binding affinity is surprisingly low (e.g. mouse E-cadherin; $K_d = 97$ μM [72]), and adhesive strength is achieved through lateral cadherin clustering. Lateral clustering does not occur at tip links, necessitating a different mechanism for high-affinity binding that can sustain substantial mechanical force. Measurements of the affinity for interactions between CDH23 and PCDH15 are eagerly awaited.

In classical cadherins, competition between *trans*- and *cis*-binding modes mediated by EC1 is thought to reduce affinity for *trans*-binding [62,73]. During adherens junction formation, such competition is mitigated by a steric mechanism resulting from ectodomain curvature [62,74]. Tip-link cadherins lack this curvature and bind heterophilically (Figure 4d), and this can be viewed as a further mechanism to increase binding affinity.

Cis *interactions by classical cadherins and tip-link cadherins*

Unlike classical cadherins, which engage in *cis* interactions by a binding surface on EC1 that interacts with EC2 [66,75], the CDH23 and PCDH15 extracellular domains form parallel homodimers with extensive lateral contacts [58]. Theoretical studies have tested the hypothesis that a classical cadherin junction is an ordered, thermodynamically condensed 2D lattice of *trans* dimers held together by *cis* interactions [76,77]. A model built on experimentally supported assumptions predicts that junction formation is a cooperative process in which initial contact between cells is mediated by *trans* dimers, creating a thermodynamic diffusion trap which promotes recruitment of monomers and formation of additional *trans* dimers. In this model, an ordered junction can form only in the presence of *cis* interactions. The extensive lateral alignment between the extracellular domains of

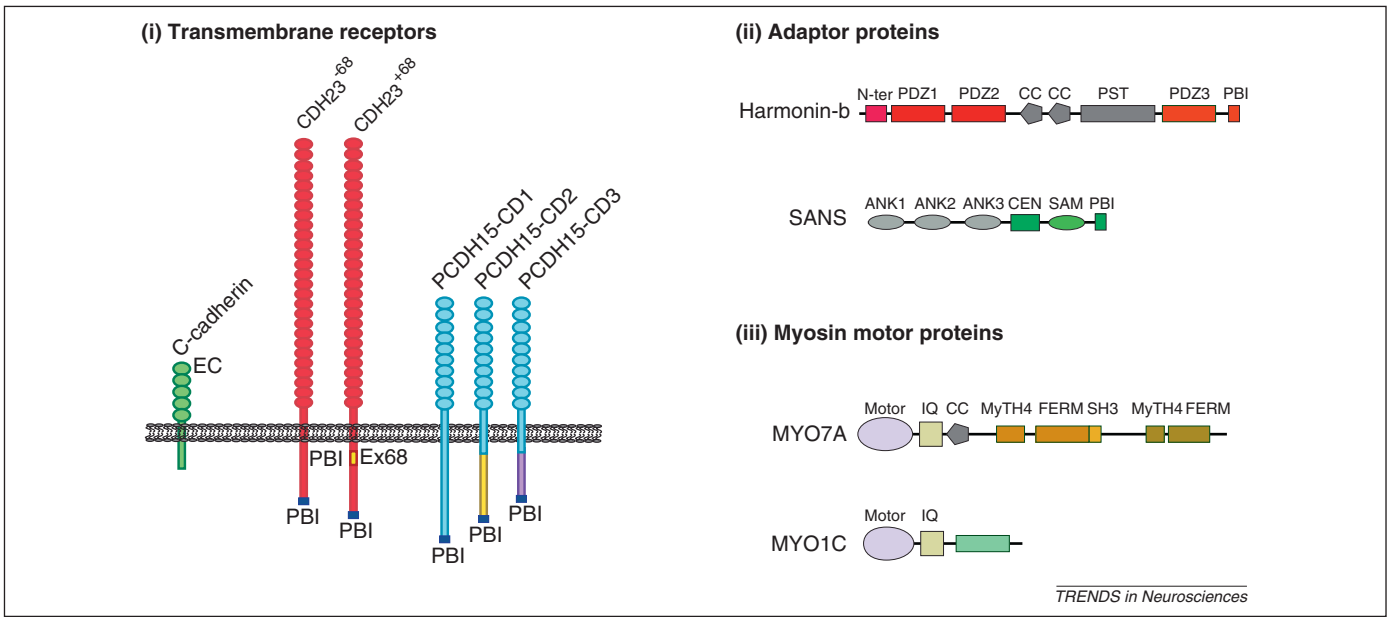

Figure 3. Molecules of transduction. The domain structure of proteins that have been implicated as components of the tip-link complex are indicated and can be grouped into three categories. **(i)** Transmembrane receptors of the cadherin superfamily (CDH23 and PCDH15) that form tip-link filaments [56–58]. The classical C-cadherin is shown for comparison to the tip-link cadherins. Note that the extracellular domains of CDH23 and PCDH15 are substantially larger than those of classical cadherins. The figure also shows different isoforms of CDH23 and PCDH15 that differ in their cytoplasmic domains. Two CDH23 isoforms have been identified in hair cells that are generated by alternative splicing of exon 68 [56,85]. For PCDH15, three prominent isoforms generated by alternative splicing (PCDH15-CD1, -CD2, and -CD3) are expressed in hair cells [57,86]. All CDH23 and PCDH15 isoforms contain consensus-binding sites for PDZ-domain proteins (PBIs) ([60] for recent review). Which isoforms of CDH23 and PCDH15 are at tip links remains to be determined. **(ii)** Adaptor proteins harmonin and sans. These adaptor proteins bind to the cytoplasmic domains of tip-link cadherins [85,94–97,114]. Harmonin can bind to the CDH23 and PCDH15 cytoplasmic domains but it co-localizes at tip links only with CDH23 [28]. Sans can bind to CDH23 and has been localized to the upper and lower ends of tip links [90,110]. **(iii)** Myosin motor proteins that are implicated in slow adaptation. Myo1c and Myo7a have been localized to the upper end of tip links but have also been reported, depending on species and experimental conditions, to be more broadly distributed in hair cells [104,105,107,110,115]. Abbreviations: Ank, ankyrin-like repeat; cc, coiled-coil domain; CEN, central sans domain; EC, extracellular cadherin repeat; FERM, protein 4.1, ezrin, radixin, moesin domain; IQ, calmodulin binding IQ domain; MyTH4, myosin tail homology 4 domain; N-ter, N-terminal domain of harmonin; PBI, PDZ binding interface; PDZ, PSD95/SAP90, Discs large, zonula occludens-1 domain; PST, proline-, serine-, threonine-rich domain; SAM, sterile alpha-motif domain; SH3, src-homology 3 domain.

CDH23 (and PCDH15) molecules might prevent additional lateral interactions that would lead to cadherin clusters – clearly an adhesion mode not desirable for tip-link formation.

Tip links as gating springs?

Since its discovery, the tip link has been an attractive candidate for the gating spring. However, high-resolution electron microscopic (EM) images suggest that tip links are stiff and buckle under strain [78]. Modeling of the classical C-cadherin extracellular domain suggests high stiffness in the presence of Ca^{2+} and limited elasticity without Ca^{2+} [79,80]. Modeling studies based on the structure of the CDH23 EC1–EC2 fragment attempted to provide estimates of the tip-link stiffness [71]. EC1 alone displayed stiffness of 710 mN/m; simulations with the first two EC domains produced the value of 570 mN/m. Assuming similar properties for the remaining EC domains, tip-link stiffness was predicted at ~40–60 mN/m. Even when Ca^{2+} was omitted in the simulations tip-link stiffness was considerable at 16 mN/m [71], far greater than the 1 mN/m measured for the gating spring.

The values obtained by modeling are burdened with several approximations. First, calculations were based on the model derived from a monomeric EC1–EC2 fragment of CDH23. Nothing is known about the structure of the remaining 25 EC domains of CDH23 and the 11 EC domains of PCDH15. Second, the membrane-proximal regions of CDH23 and PCDH15 (~100 amino acids) fold into an unknown structure. Finally, EM studies suggest that the two strands of the tip-link filament separate close to the upper membrane-insertion point [78]. Such separation could lead to substantial structural flexibility.

Mechanical properties of tip-link cadherins have not been studied, but the nanomechanics of C-cadherin has been experimentally analyzed [80]. Single-molecule force spectroscopy confirms Ca^{2+} induces ectodomain rigidification. When force is applied in the presence of 1 mM Ca^{2+}, EC-domain unfolding requires ~186 pN and stretches the molecule by ~34.2 nm. This force peak is preceded by a smaller one. At ~143 pN C-cadherin stretches by ~2.7 nm as a single Ca^{2+} binding site unfolds. Without Ca^{2+} the EC domains are less stable and unfold at ~83 pN [80]. At 0.1 mM Ca^{2+}, the unfolding force is ~90 pN, significantly lower than in 1 mM Ca^{2+} [80]. Notably, the Ca^{2+} concentration of the endolymph varies tonotopically and reaches low levels (~20 μM) [81,82]. *Trans* interactions between CDH23 and PCDH15 are not disrupted even at 100 μM Ca^{2+} [58], but low local Ca^{2+} concentration might affect the mechanical properties of tip-links.

Based on the above studies, it seems plausible that the gating spring is formed by a molecule distinct from tip-link cadherins, although it does not necessarily have to be a protein. The plasma membrane near the lower tip-link insertion points appears to be under tension and pulls away from the cytoskeleton; this morphological feature is lost when tip links are broken [8,78,83]. Perhaps, forces that are too small to rupture or stretch tip links can deform the lipid bilayer. Interestingly, the stiffness module of the plasma membrane of the cell body in OHCs is ~1 mN/m [84], a

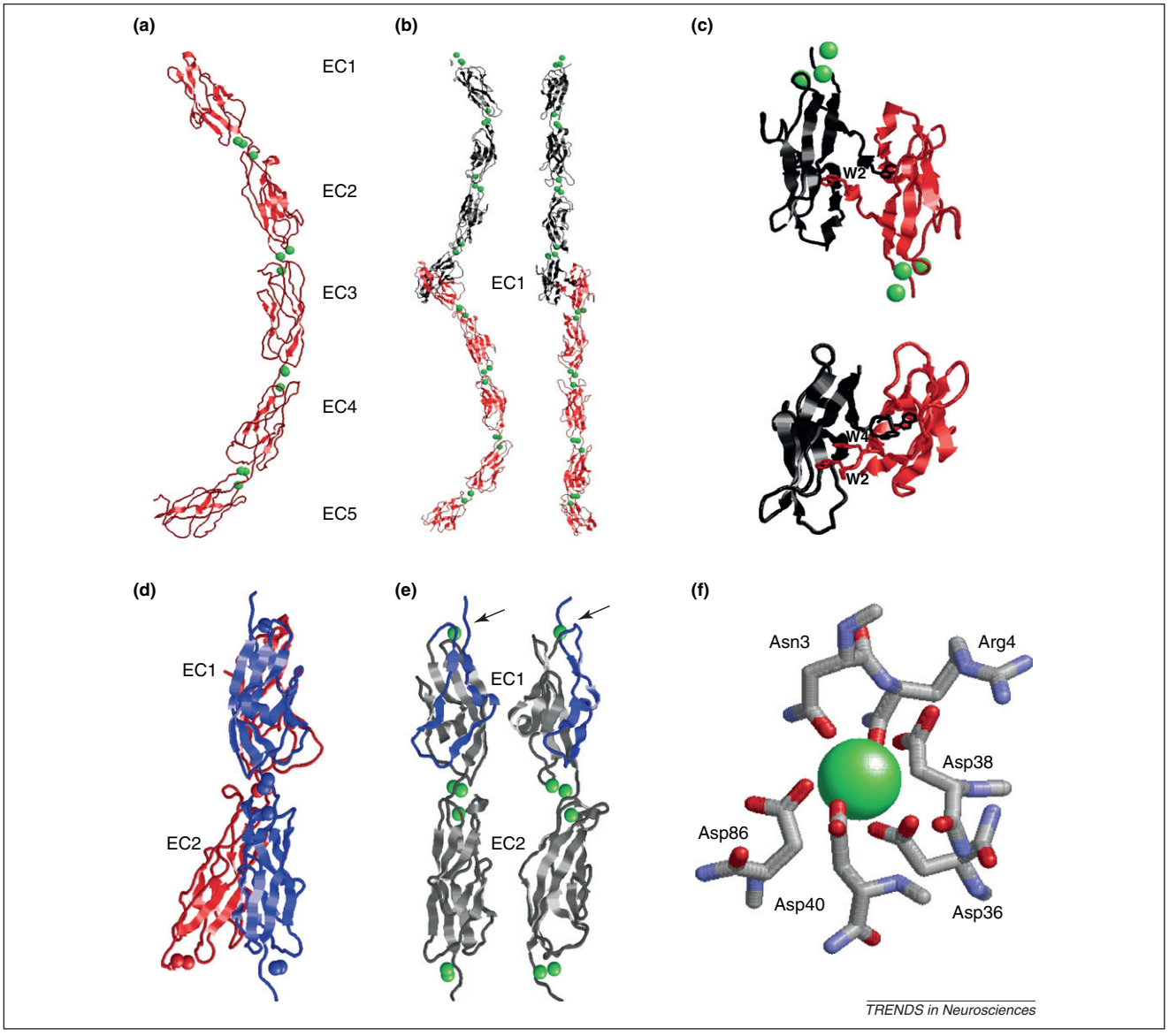

Figure 4. Structural features of the extracellular domains of classical cadherins and Cdh23. The figures summarize crystallographic data for classical cadherins and tip-link cadherins. **(a)** The entire *Xenopus laevis* C-cadherin extracellular domain (red) in the Ca^{2+} (green) -bound state is shown. Note the five extracellular cadherin repeats (EC1–5), the three Ca^{2+} ions that are bound between each of the EC domains, and the curvature of the ectodomain [66]. **(b)** Adhesive *trans* dimer of murine E-cadherin [116]. Individual E-cadherin extracellular domains (red and black) emanate from opposing directions. The *trans* binding surface is located in the EC1 domain. Side-view (left) reveals the characteristic curvature of the monomers, which appear straight when rotated by 90° (right). **(c)** The N-terminal EC1 domains of classical cadherins that engage in *trans* interactions are depicted. The molecules form the so-called strand-swapped dimers. Classical type I cadherins such as murine E-cadherin (upper) contain in EC1 one key Trp residue (W2) that fits into a binding pocket in EC1 of its binding partner [116]. Classical type II cadherins such as chicken MN-cadherin (lower) contain two Trp residues (W2 and W4) that fit into two binding pockets on EC1 of the binding partner [69]. **(d)** Crystallographic structure of the EC1–EC2 domain of murine CDH23 (blue) [70,71]. The classic cadherin fold with Ca^{2+} ions (blue dots) between EC1 and EC2 is maintained. Superimposition of EC1–EC2 of C-cadherin (red) highlights the straight alignment of CDH23 EC1–EC2 compared to the curvature of C- cadherin [66,70]. **(e)** Structure of the EC1–EC2 domains of two parallel CDH23 molecules. Note that only monomeric structures have been crystallized. The contact surface between EC domains that are aligned in parallel remains to be determined. Ca^{2+} ions (green dots) are indicated. Note the presence of a Ca^{2+} ion at the extreme N-terminus of CDH23 that is not bound by classical cadherins. The strands formed by amino acids 1–4 are clamped down in a loop (blue) by the coordinate bond between Asn3, Arg4, Asp36, Asp38, Asp40 and Ca^{2+} to form a large exposed area on the surface of EC1. Mutations in Asn3 and Arg4 reduce CDH23 binding to PCDH15 [70]. **(f)** Detailed view of the amino acids in CDH23 that coordinate the N-terminal Ca^{2+} [70,71]. Structures were generated in RasMol (http://www.umass.edu/microbio/rasmol/) using protein coordinates from the Protein Data Bank (PDB) database (www.pdb.org).

value strikingly similar to the gating-spring stiffness. We do not know the mechanical properties of the stereociliary membrane, but one possibility is that force-induced membrane deformation could account for the gating spring.

Cytoplasmic components of the tip-link complex

Cytoplasmic domains of tip-link cadherins

The cytoplasmic domains of classical cadherins harbor binding sites for many proteins, including β-catenin and p120 catenin [68]. The cytoplasmic domains of tip-link cadherins show no sequence homology to classical cadherins, suggesting that they recruit different proteins. Both the CDH23 and PCDH15 cytoplasmic domains are also alternatively spliced, providing additional diversity. Two cytoplasmic splice variants have been described for CDH23. The longer isoform contains an insert of 35 amino acids and is specifically expressed in hair cells [56,85]. For PCDH15, three prominent isoforms named CD1, CD2, and CD3 have been described which differ in their cytoplasmic domains; all three are expressed in hair cells [57,86]. However, which isoforms of CDH23 and PCDH15 contribute to the tip link is unclear (discussed below).

Binding partners for CDH23 and PCDH15 and hair-bundle development

The identification of binding partners for the cytoplasmic domains of CDH23 and PCDH15 has been facilitated by the study of genes linked to deafness. Mutations in *CDH23* and *PCDH15* lead to Usher syndrome type I (USH1) [47,49–51], a severe form of deaf-blindness. The disease is also caused by mutations in the genes encoding the molecular motor myosin 7a (Myo7a), and the adaptor proteins harmonin and sans (scaffold protein containing ankyrin repeats and SAM domain) [87–89]. Mutations in the murine orthologs of the human genes lead to defects in hair-bundle morphology, suggesting that USH1 proteins act in a common pathway [48,52,54,90–94]. This notion is supported by *in vitro* studies which show that USH1 proteins bind to each other. Harmonin, sans and Myo7a bind *in vitro* to all USH1 proteins; harmonin and sans also interact homophilically; finally, harmonin and Myo7a bind to F-actin (Figure 3 for protein domain structures) [85,94–101].

USH1 proteins are broadly distributed in developing hair bundles, where they form the linkages that connect the stereocilia to each other and to the single kinocilium (which is present in developing cochlear hair cells but degenerates as the cells mature) ([3,4] for recent reviews). Intriguingly, alternative splicing regulates the function of PCDH15 in hair cells. PCDH15-CD2-deficient mice, but not mice lacking PCDH15-CD1 or -CD3, lack kinociliary links and develop hair bundles with abnormal polarity [86]. PCDH15-CD2 is abundantly expressed in the kinocilium, whereas CDH23 is expressed in the adjacent stereocilia, suggesting that kinociliary links are heteromeric complexes consisting of CDH23 and PCDH15 [59,86]. Therefore, kinociliary links resemble tip links in composition, except with reversed polarity in CDH23 and PCDH15 localization relative to the hair-bundle polarity axis [58,59]. PCDH15-CD2 in kinocilia might recruit CDH23 (which does not traffic into kinocilia) to the longest stereocilia next to the kinocilium. This would lead to the formation of kinociliary links. Some CDH23 in the longest stereocilia might then bind to PCDH15 in the next shorter row of stereocilia, establishing opposite polarity in tip links.

Binding partners for CDH23 at tip links

The tip-link localization of CDH23 and PCDH15 suggested that their binding partners also function in mechanotransduction. This was initially demonstrated for harmonin-b, a harmonin isoform that binds to CDH23, Myo7a, sans and F-actin [85,95–98,100,101] (Figure 5). In adult hair cells, harmonin-b is localized to the upper tip-link density (UTLD) [28], which can be visualized by transmission EM as a density below the membrane at the upper tip-link insertion-point [102]. *Deaf circler* (*dfcr*) mice, which carry a harmonin-b mutation that prevents interaction with F-actin [91], preserve their tip links but lack UTLDs [28]. Gating of transduction channels throughout the hair bundle is less well-coordinated in the mutants, and transducer current activation and adaptation are slowed [28]. Harmonin-b might connect the tip link to the cytoskeleton and regulate the activity of the slow adaptation motor, thereby establishing tension in the transduction machinery. Analyses of transducer currents in *dfcr2J* mice, which entirely lack harmonin-b, have similarly implicated harmonin in regulating the slow adaptation motor [103].

The most prominent current model proposes that the slow adaptation motor is formed by a cluster of myosin-1c (Myo1c) motor proteins at the UTLD ([24] for recent review). In support of this model, Myo1c in frogs is concentrated close to the UTLD [104,105]; its inactivation dramatically affects channel open probability at rest and adaptation [32,106]. The close proximity of Myo1c and harmonin-b at UTLDs and the demonstration that Myo1c forms a protein complex with CDH23 [56] suggest that harmonin-b might affect Myo1c function. However, as outlined above (also Figure 2c), Ca^{2+} enters stereocilia close to the lower end of tip links [6], raising questions as to the mechanism by which Ca^{2+}regulates the slow adaptation motor at the upper tip-link end. Furthermore, a recent study shows that in IHC of mammals, Myo1c is distributed along the length of stereocilia [107]. Therefore, the function of Myo1c in adaptation needs further study.

Myo7a has emerged as a second candidate for the slow adaptation motor. Accordingly, mice with a mutation in Myo7a show defects in transduction and altered adaptation [108]. Immunolocalization studies suggested that Myo7a in frog hair cells is concentrated in the cell body and at the base of the hair bundle [109], but a study in mice has revealed additional expression at the UTLD [110]. The same study also localized sans to the UTLD [110]. Biochemical and crystallographic data show that CDH23, harmonin, Myo7a, and sans form a multimeric protein complex (Figure 5) [85,95–98,100,101,110]. Notably, harmonin binds through multiple surfaces to CDH23 [85,95–98,100,101,110], leading to a binding affinity that is far greater than that measured for interactions between other PDZ-domain proteins and their interaction partners [96]. Inactivation of sans in mice leads to a reduction in transducer current and loss of tip links [90]. Perhaps the protein complex at UTLDs is unstable without sans.

Binding partners for PCDH15 at tip links

Little is known about the putative protein complex at the lower tip-link end that includes PCDH15 and the elusive transduction channel. Immunolocalization studies initially suggested that the PCDH15-CD3 isoform is present at the lower tip-link end [57]. However, tip links form in mice individually lacking PCDH15-CD1, -CD2, or -CD3, indicating that several of these isoforms function redundantly at tip links [86]. Notably, all PCDH15 isoforms share a proline-rich membrane-proximal region and contain a C-terminal binding site for PDZ-domain proteins (Figure 3) [57]. They might therefore recruit similar proteins through these shared domains. Several proteins such as whirlin, Myo3a, Myo15, and espin1 have been localized to the tips of stereocilia; functional studies implicate them in regulating stereociliary elongation ([4] for a recent review). The extent to which these proteins participate in regulating transduction channels is unclear. Mice with a mutation in Myo15 show altered transduction [111,112], but morphological hair-bundle defects make it difficult to ascertain direct effects of Myo15 on transduction. As pointed out above, structural studies and immunolocalization studies have placed sans at the UTLD, but a recent study has concluded that sans is located close to

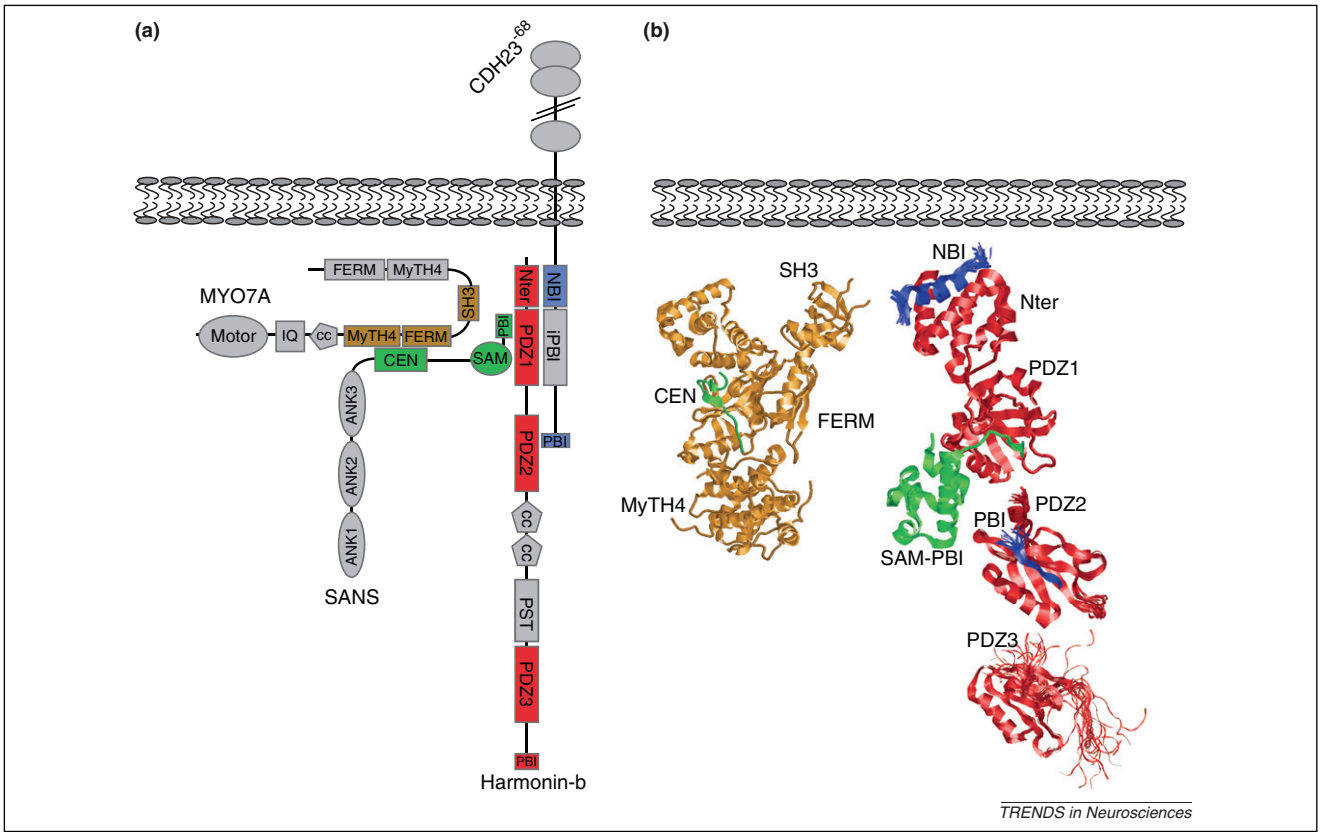

Figure 5. Structural aspects of the UTLD complex emerging from crystallographic and biochemical studies. **(a,b)** Modeling of the interactions between proteins at the UTLD. In **(a)** a model of the interaction surfaces is provided that is based on biochemical data and, where available, on structural information [85,94–101]. In **(b)** the known crystal structures are shown, except for an internal binding motif for PDZ-domain proteins (NBI) of CDH23, which was fitted artificially into its N-terminal binding site on harmonin. Protein-domains in **(a)** are color-coded to match the structures in **(b)**. Abbreviations are as in Figure 3. Note that we present here a partial representation not considering all interactions revealed by biochemical data. For example, Myo7a can also bind to harmonin and CDH23 [93,105], but these complexes have not yet been crystallized. Structures were generated as described in Figure 4.

the LTLD [90]. Sans might therefore also play a role in regulating transduction at the lower tip-link region.

Concluding remarks

Building on a solid biophysical foundation, researchers have started to identify the molecules required for mechanotransduction by hair cells. Two themes emerge: asymmetry and evolution of special features required for force transmission.

Box 1. Outstanding questions

- What is the molecular identity of the mechanotransduction channel?
- What are the mechanical properties of tip links, and what is the atomic structure of the adhesion interface between CDH23 and PCDH15?
- Which molecule(s) form the gating spring for the transducer channel?
- What is the mechanism of fast adaptation? What is the mechanism of slow adaptation and what roles do Myo1c and Myo7a play in this process? Are other myosin motor proteins involved?
- What is the full complement of proteins at the upper and lower end of tip links and how do they regulate tip-link function in mechanotransduction?
- How is the exquisite polarity of CDH23 and PCDH15 at tip links achieved, and how are proteins such as the transduction channel and harmonin targeted to opposite ends of the tip link?
- Which mechanisms define the numbers and rows of stereocilia and their organ-pipe arrangement?
- Which signaling mechanisms establish precise polarity of the hair bundle in the apical surface of a hair cell?

Asymmetry is evident in the composition of the tip-link, in the proteins recruited by the cytoplasmic domains of tip-link cadherins, and in the localization of the transduction channel (Figure 2). Specialized features for force transmission are probably the new binding surface between CDH23 and PCDH15, and the high-affinity binding mode between CDH23 and harmonin. However, there are several important outstanding questions (Box 1). The most intriguing issue, of course, is the identity of the transduction channel.

Acknowledgments

We thank members of the laboratory and Dr. Peter Gillespie (Oregon Hearing Research Center and Vollum Institute) for comments. This work was supported by funding from the National Institutes of Health (DC005965, DC007704), the California Institute of Regenerative Medicine, the Skaggs Institute for Chemical Biology, the Bundy Foundation, and the Dorris Neuroscience Center.

References

1 Gillespie, P.G. and Muller, U. (2009) Mechanotransduction by hair cells: models, molecules, and mechanisms. *Cell* 139, 33–44
2 Meyer, A.C. and Moser, T. (2010) Structure and function of cochlear afferent innervation. *Curr. Opin. Otolaryngol. Head Neck Surg.* 18, 441–446
3 Richardson, G.P. *et al.* (2011) How the genetics of deafness illuminates auditory physiology. *Ann. Rev. Physiol.* 73, 311–334
4 Schwander, M. *et al.* (2010) Review series: the cell biology of hearing. *J. Cell Biol.* 190, 9–20
5 Pickles, J.O. *et al.* (1984) Cross-links between stereocilia in the guinea pig organ of Corti, and their possible relation to sensory transduction. *Hear. Res.* 15, 103–112

6 Beurg, M. *et al.* (2009) Localization of inner hair cell mechanotransducer channels using high-speed calcium imaging. *Nat. Neurosci.* 12, 553–558
7 Denk, W. *et al.* (1995) Calcium imaging of single stereocilia in hair cells: localization of transduction channels at both ends of tip links. *Neuron* 15, 1311–1321
8 Assad, J.A. *et al.* (1991) Tip-link integrity and mechanical transduction in vertebrate hair cells. *Neuron* 7, 985–994
9 Zhao, Y. *et al.* (1996) Regeneration of broken tip links and restoration of mechanical transduction in hair cells. *Proc. Natl. Acad. Sci. U.S.A.* 93, 15469–15474
10 Markin, V.S. and Hudspeth, A.J. (1995) Gating-spring models of mechanoelectrical transduction by hair cells of the internal ear. *Annu. Rev. Biophys. Biomol. Struct.* 24, 59–83
11 Rhode, W.S. and Geisler, C.D. (1967) Model of the displacement between opposing points on the tectorial membrane and reticular lamina. *J. Acoust. Soc. Am.* 42, 185–190
12 Corey, D.P. and Hudspeth, A.J. (1983) Kinetics of the receptor current in bullfrog saccular hair cells. *J. Neurosci.* 3, 962–976
13 Crawford, A.C. *et al.* (1989) Activation and adaptation of transducer currents in turtle hair cells. *J. Physiol.* 419, 405–434
14 Flock, A. *et al.* (1977) Studies on the sensory hairs of receptor cells in the inner ear. *Acta Otolaryngol.* 83, 85–91
15 Hudspeth, A.J. and Corey, D.P. (1977) Sensitivity, polarity, and conductance change in the response of vertebrate hair cells to controlled mechanical stimuli. *Proc. Natl. Acad. Sci. U.S.A.* 74, 2407–2411
16 Karavitaki, K.D. and Corey, D.P. (2010) Sliding adhesion confers coherent motion to hair cell stereocilia and parallel gating to transduction channels. *J. Neurosci.* 30, 9051–9063
17 Kozlov, A.S. *et al.* (2007) Coherent motion of stereocilia assures the concerted gating of hair-cell transduction channels. *Nat. Neurosci.* 10, 87–92
18 Kozlov, A.S. *et al.* (2011) Forces between clustered stereocilia minimize friction in the ear on a subnanometre scale. *Nature* 474, 376–379
19 Ricci, A.J. *et al.* (2005) The transduction channel filter in auditory hair cells. *J. Neurosci.* 25, 7831–7839
20 Shotwell, S.L. *et al.* (1981) Directional sensitivity of individual vertebrate hair cells to controlled deflection of their hair bundles. *Ann. N. Y. Acad. Sci.* 374, 1–10
21 Howard, J. and Hudspeth, A.J. (1988) Compliance of the hair bundle associated with gating of mechanoelectrical transduction channels in the bullfrog's saccular hair cell. *Neuron* 1, 189–199
22 Ricci, A.J. *et al.* (2002) Mechanisms of active hair bundle motion in auditory hair cells. *J. Neurosci.* 22, 44–52
23 Fettiplace, R. and Ricci, A.J. (2003) Adaptation in auditory hair cells. *Curr. Opin. Neurobiol.* 13, 446–451
24 Gillespie, P.G. and Cyr, J.L. (2004) Myosin-1c, the hair cell's adaptation motor. *Ann. Rev. Physiol.* 66, 521–545
25 Hudspeth, A.J. (2008) Making an effort to listen: mechanical amplification in the ear. *Neuron* 59, 530–545
26 Eatock, R.A. *et al.* (1987) Adaptation of mechanoelectrical transduction in hair cells of the bullfrog's sacculus. *J. Neurosci.* 7, 2821–2836
27 Crawford, A.C. *et al.* (1991) The actions of calcium on the mechano-electrical transducer current of turtle hair cells. *J. Physiol.* 434, 369–398
28 Grillet, N. *et al.* (2009) Harmonin mutations cause mechanotransduction defects in cochlear hair cells. *Neuron* 62, 375–387
29 Kennedy, H.J. *et al.* (2003) Fast adaptation of mechanoelectrical transducer channels in mammalian cochlear hair cells. *Nat. Neurosci.* 6, 832–836
30 Ricci, A.J. and Fettiplace, R. (1997) The effects of calcium buffering and cyclic AMP on mechano-electrical transduction in turtle auditory hair cells. *J. Physiol.* 501 (Pt 1), 111–124
31 Stauffer, E.A. and Holt, J.R. (2007) Sensory transduction and adaptation in inner and outer hair cells of the mouse auditory system. *J. Neurophysiol.* 98, 3360–3369
32 Stauffer, E.A. *et al.* (2005) Fast adaptation in vestibular hair cells requires Myosin-1c activity. *Neuron* 47, 541–553
33 Vollrath, M.A. and Eatock, R.A. (2003) Time course and extent of mechanotransducer adaptation in mouse utricular hair cells: comparison with frog saccular hair cells. *J. Neurophysiol.* 90, 2676–2689
34 Waguespack, J. *et al.* (2007) Stepwise morphological and functional maturation of mechanotransduction in rat outer hair cells. *J. Neurosci.* 27, 13890–13902
35 Wu, Y.C. *et al.* (1999) Two components of transducer adaptation in auditory hair cells. *J. Neurophysiol.* 82, 2171–2181
36 Bozovic, D. and Hudspeth, A.J. (2003) Hair-bundle movements elicited by transepithelial electrical stimulation of hair cells in the sacculus of the bullfrog. *Proc. Natl. Acad. Sci. U.S.A.* 100, 958–963
37 Martin, P. *et al.* (2003) Spontaneous oscillation by hair bundles of the bullfrog's sacculus. *J. Neurosci.* 23, 4533–4548
38 Assad, J.A. and Corey, D.P. (1992) An active motor model for adaptation by vertebrate hair cells. *J. Neurosci.* 12, 3291–3309
39 Howard, J. and Hudspeth, A.J. (1987) Mechanical relaxation of the hair bundle mediates adaptation in mechanoelectrical transduction by the bullfrog's saccular hair cell. *Proc. Natl. Acad. Sci. U.S.A.* 84, 3064–3068
40 Corey, D.P. and Hudspeth, A.J. (1979) Ionic basis of the receptor potential in a vertebrate hair cell. *Nature* 281, 675–677
41 Ohmori, H. (1985) Mechano-electrical transduction currents in isolated vestibular hair cells of the chick. *J. Physiol.* 359, 189–217
42 Beurg, M. *et al.* (2006) A large-conductance calcium-selective mechanotransducer channel in mammalian cochlear hair cells. *J. Neurosci.* 26, 10992–11000
43 Ricci, A.J. *et al.* (2003) Tonotopic variation in the conductance of the hair cell mechanotransducer channel. *Neuron* 40, 983–990
44 Farris, H.E. *et al.* (2004) Probing the pore of the auditory hair cell mechanotransducer channel in turtle. *J. Physiol.* 558, 769–792
45 Cueva, J.G. *et al.* (2007) Nanoscale organization of the MEC-4 DEG/ENaC sensory mechanotransduction channel in *Caenorhabditis elegans* touch receptor neurons. *J. Neurosci.* 27, 14089–14098
46 Kung, C. *et al.* (2010) Mechanosensitive channels in microbes. *Ann. Rev. Microbiol.* 64, 313–329
47 Ahmed, Z.M. *et al.* (2001) Mutations of the protocadherin gene PCDH15 cause Usher syndrome type 1F. *Am. J. Hum. Genet.* 69, 25–34
48 Alagramam, K.N. *et al.* (2001) The mouse Ames *waltzer* hearing-loss mutant is caused by mutation of *Pcdh15*, a novel protocadherin gene. *Nat. Genet.* 27, 99–102
49 Alagramam, K.N. *et al.* (2001) Mutations in the novel protocadherin PCDH15 cause Usher syndrome type 1F. *Hum. Mol. Genet.* 10, 1709–1718
50 Bolz, H. *et al.* (2001) Mutation of *CDH23*, encoding a new member of the cadherin gene family, causes Usher syndrome type 1D. *Nat. Genet.* 27, 108–112
51 Bork, J.M. *et al.* (2001) Usher syndrome 1D and nonsyndromic autosomal recessive deafness DFNB12 are caused by allelic mutations of the novel cadherin-like gene *CDH23*. *Am. J. Hum. Genet.* 68, 26–37
52 Di Palma, F. *et al.* (2001) Mutations in *Cdh23*, encoding a new type of cadherin, cause stereocilia disorganization in *waltzer*, the mouse model for Usher syndrome type 1D. *Nat. Genet.* 27, 103–107
53 Wada, T. *et al.* (2001) A point mutation in a cadherin gene, *Cdh23*, causes deafness in a novel mutant, *Waltzer* mouse niigata. *Biochem. Biophys. Res. Commun.* 283, 113–117
54 Wilson, S.M. *et al.* (2001) Mutations in *Cdh23* cause nonsyndromic hearing loss in *waltzer* mice. *Genomics* 74, 228–233
55 Sollner, C. *et al.* (2004) Mutations in cadherin 23 affect tip links in zebrafish sensory hair cells. *Nature* 428, 955–959
56 Siemens, J. *et al.* (2004) Cadherin 23 is a component of the tip link in hair-cell stereocilia. *Nature* 428, 950–955
57 Ahmed, Z.M. *et al.* (2006) The tip-link antigen, a protein associated with the transduction complex of sensory hair cells, is protocadherin-15. *J. Neurosci.* 26, 7022–7034
58 Kazmierczak, P. *et al.* (2007) Cadherin 23 and protocadherin 15 interact to form tip-link filaments in sensory hair cells. *Nature* 449, 87–91
59 Goodyear, R.J. *et al.* (2010) Asymmetric distribution of cadherin 23 and protocadherin 15 in the kinocilial links of avian sensory hair cells. *J. Comp. Neurol.* 518, 4288–4297
60 Muller, U. (2008) Cadherins and mechanotransduction by hair cells. *Curr. Opin. Cell Biol.* 20, 557–566
61 Niessen, C.M. *et al.* (2011) Tissue organization by cadherin adhesion molecules: dynamic molecular and cellular mechanisms of morphogenetic regulation. *Physiol. Rev.* 91, 691–731
62 Shapiro, L. and Weis, W.I. (2009) Structure and biochemistry of cadherins and catenins. *Cold Spring Harb. Perspect. Biol.* 1, a003053
63 Yagi, T. and Takeichi, M. (2000) Cadherin superfamily genes: functions, genomic organization, and neurologic diversity. *Genes Dev.* 14, 1169–1180

64 Nelson, W.J. (2008) Regulation of cell–cell adhesion by the cadherin–catenin complex. *Biochem. Soc. Trans.* 36, 149–155
65 Oda, H. and Takeichi, M. (2011) Evolution: structural and functional diversity of cadherin at the adherens junction. *J. Cell Biol.* 193, 1137–1146
66 Boggon, T.J. *et al.* (2002) C-cadherin ectodomain structure and implications for cell adhesion mechanisms. *Science* 296, 1308–1313
67 Haussinger, D. *et al.* (2004) Proteolytic E-cadherin activation followed by solution NMR and X-ray crystallography. *EMBO J.* 23, 1699–1708
68 Zhang, Y. *et al.* (2009) Resolving cadherin interactions and binding cooperativity at the single-molecule level. *Proc. Natl. Acad. Sci. U.S.A.* 106, 109–114
69 Patel, S.D. *et al.* (2006) Type II cadherin ectodomain structures: implications for classical cadherin specificity. *Cell* 124, 1255–1268
70 Elledge, H.M. *et al.* (2010) Structure of the N terminus of cadherin 23 reveals a new adhesion mechanism for a subset of cadherin superfamily members. *Proc. Natl. Acad. Sci. U S.A.* 107, 10708–10712
71 Sotomayor, M. *et al.* (2010) Structural determinants of cadherin-23 function in hearing and deafness. *Neuron* 66, 85–100
72 Katsamba, P. *et al.* (2009) Linking molecular affinity and cellular specificity in cadherin-mediated adhesion. *Proc. Natl. Acad. Sci. U.S.A.* 106, 11594–11599
73 Chen, C.P. *et al.* (2005) Specificity of cell-cell adhesion by classical cadherins: Critical role for low-affinity dimerization through beta-strand swapping. *Proc. Natl. Acad. Sci. U.S.A.* 102, 8531–8536
74 Pokutta, S. *et al.* (1994) Conformational changes of the recombinant extracellular domain of E-cadherin upon calcium binding. *Eur. J. Biochem.* 223, 1019–1026
75 Harrison, O.J. *et al.* (2011) The extracellular architecture of adherens junctions revealed by crystal structures of type I cadherins. *Structure* 19, 244–256
76 Wu, Y. *et al.* (2011) Transforming binding affinities from three dimensions to two with application to cadherin clustering. *Nature* 475, 510–513
77 Wu, Y. *et al.* (2010) Cooperativity between *trans* and *cis* interactions in cadherin-mediated junction formation. *Proc. Natl. Acad. Sci. U.S.A.* 107, 17592–17597
78 Kachar, B. *et al.* (2000) High-resolution structure of hair-cell tip links. *Proc. Natl. Acad. Sci. U.S.A.* 97, 13336–13341
79 Sotomayor, M. and Schulten, K. (2008) The allosteric role of the Ca^{2+} switch in adhesion and elasticity of C-cadherin. *Biophys. J.* 94, 4621–4633
80 Oroz, J. *et al.* (2011) Nanomechanics of the cadherin ectodomain: 'canalization' by Ca^{2+} binding results in a new mechanical element. *J. Biol. Chem.* 286, 9405–9418
81 Bosher, S.K. and Warren, R.L. (1978) Very low calcium content of cochlear endolymph, an extracellular fluid. *Nature* 273, 377–378
82 Salt, A.N. *et al.* (1989) Calcium gradients in inner ear endolymph. *Am. J. Otolaryngol.* 10, 371–375
83 Schwander, M. *et al.* (2009) A mouse model for nonsyndromic deafness (DFNB12) links hearing loss to defects in tip links of mechanosensory hair cells. *Proc. Natl. Acad. Sci. U.S.A.* 106, 5252–5257
84 Tolomeo, J.A. *et al.* (1996) Mechanical properties of the lateral cortex of mammalian auditory outer hair cells. *Biophys. J.* 71, 421–429
85 Siemens, J. *et al.* (2002) The Usher syndrome proteins cadherin 23 and harmonin form a complex by means of PDZ-domain interactions. *Proc. Natl. Acad. Sci. U.S.A.* 99, 14946–14951
86 Webb, S.W. *et al.* (2011) Regulation of PCDH15 function in mechanosensory hair cells by alternative splicing of the cytoplasmic domain. *Development* 138, 1607–1617
87 Verpy, E. *et al.* (2000) A defect in harmonin, a PDZ domain-containing protein expressed in the inner ear sensory hair cells, underlies Usher syndrome type 1C. *Nat. Genet.* 26, 51–55
88 Weil, D. *et al.* (1995) Defective myosin VIIA gene responsible for Usher syndrome type 1B. *Nature* 374, 60–61
89 Weil, D. *et al.* (2003) Usher syndrome type I G (USH1G) is caused by mutations in the gene encoding SANS, a protein that associates with the USH1C protein, harmonin. *Hum. Mol. Genet.* 12, 463–471
90 Caberlotto, E. *et al.* (2011) Usher type 1G protein sans is a critical component of the tip-link complex, a structure controlling actin polymerization in stereocilia. *Proc. Natl. Acad. Sci. U.S.A.* 108, 5825–5830
91 Johnson, K.R. *et al.* (2003) Mouse mo of USH1C and DFNB18: phenotypic and molecular analyses of two new spontaneous mutations of the *Ush1c* gene. *Hum. Mol. Genet.* 12, 3075–3086
92 Lefevre, G. *et al.* (2008) A core cochlear phenotype in USH1 mouse mutants implicates fibrous links of the hair bundle in its cohesion, orientation and differential growth. *Development* 135, 1427–1437
93 Self, T. *et al.* (1998) Shaker-1 mutations reveal roles for myosin VIIA in both development and function of cochlear hair cells. *Development* 125, 557–566
94 Senften, M. *et al.* (2006) Physical and functional interaction between protocadherin 15 and myosin VIIa in mechanosensory hair cells. *J. Neurosci.* 26, 2060–2071
95 Adato, A. *et al.* (2005) Interactions in the network of Usher syndrome type 1 proteins. *Hum. Mol. Genet.* 14, 347–356
96 Bahloul, A. *et al.* (2010) Cadherin-23, myosin VIIa and harmonin, encoded by Usher syndrome type I genes, form a ternary complex and interact with membrane phospholipids. *Hum. Mol. Genet.* 19, 3557–3565
97 Boeda, B. *et al.* (2002) Myosin VIIa, harmonin and cadherin 23, three Usher I gene products that cooperate to shape the sensory hair cell bundle. *EMBO J.* 21, 6689–6699
98 Pan, L. *et al.* (2009) Assembling stable hair cell tip link complex via multidentate interactions between harmonin and cadherin 23. *Proc. Natl. Acad. Sci. U.S.A.* 106, 5575–5580
99 Reiners, J. *et al.* (2005) Photoreceptor expression of the Usher syndrome type 1 protein protocadherin 15 (USH1F) and its interaction with the scaffold protein harmonin (USH1C). *Mol. Vis.* 11, 347–355
100 Wu, L. *et al.* (2011) Structure of MyTH4-FERM domains in myosin VIIa tail bound to cargo. *Science* 331, 757–760
101 Yan, J. *et al.* (2010) The structure of the harmonin/sans complex reveals an unexpected interaction mode of the two Usher syndrome proteins. *Proc. Natl. Acad. Sci. U.S.A.* 107, 4040–4045
102 Furness, D.N. and Hackney, C.M. (1985) Cross-links between stereocilia in the guinea pig cochlea. *Hear. Res.* 18, 177–188
103 Michalski, N. *et al.* (2009) Harmonin-b, an actin-binding scaffold protein, is involved in the adaptation of mechanoelectrical transduction by sensory hair cells. *Pflugers Arch.* 459, 115–130
104 Garcia, J.A. *et al.* (1998) Localization of myosin-Ibeta near both ends of tip links in frog saccular hair cells. *J. Neurosci.* 18, 8637–8647
105 Steyger, P.S. *et al.* (1998) Myosin Ibeta is located at tip link anchors in vestibular hair bundles. *J. Neurosci.* 18, 4603–4615
106 Holt, J.R. *et al.* (2002) A chemical–genetic strategy implicates myosin-1c in adaptation by hair cells. *Cell* 108, 371–381
107 Schneider, M.E. *et al.* (2006) A new compartment at stereocilia tips defined by spatial and temporal patterns of myosin IIIa expression. *J. Neurosci.* 26, 10243–10252
108 Kros, C.J. *et al.* (2002) Reduced climbing and increased slipping adaptation in cochlear hair cells of mice with Myo7a mutations. *Nat. Neurosci.* 5, 41–47
109 Hasson, T. (1997) Unconventional myosins, the basis for deafness in mouse and man. *Am. J. Hum. Genet.* 61, 801–805
110 Grati, M. and Kachar, B. (2011) Myosin VIIa and sans localization at stereocilia upper tip-link density implicates these Usher syndrome proteins in mechanotransduction. *Proc. Natl. Acad. Sci. U.S.A.* 108, 11476–11481
111 Stepanyan, R. *et al.* (2006) Auditory mechanotransduction in the absence of functional myosin-XVa. *J. Physiol.* 576, 801–808
112 Stepanyan, R. and Frolenkov, G.I. (2009) Fast adaptation and Ca2+ sensitivity of the mechanotransducer require myosin-XVa in inner but not outer cochlear hair cells. *J. Neurosci.* 29, 4023–4034
113 Goodyear, R.J. *et al.* (2005) Development and properties of stereociliary link types in hair cells of the mouse cochlea. *J. Comp. Neurol.* 485, 75–85
114 Reiners, J. *et al.* (2006) Molecular basis of human Usher syndrome: deciphering the meshes of the Usher protein network provides insights into the pathomechanisms of the Usher disease. *Exp. Eye Res.* 83, 97–119
115 Hasson, T. *et al.* (1997) Unconventional myosins in inner-ear sensory epithelia. *J. Cell Biol.* 137, 1287–1307
116 Harrison, O.J. *et al.* (2010) Two-step adhesive binding by classical cadherins. *Nat. Struct. Mol. Biol.* 17, 348–357